Al-Azhar Bull. Sci. Vol. 22, No. 2 (Dec.): pp. 1-32, 2011.

EVOLUTION OF THE TALC-CARBONATE ROCKS IN UMM RILAN OPHIOLITE, SOUTH EASTERN DESERT, EGYPT: IMPLICATION FROM MINERALOGY, PETROGRAPHY, GEOCHEMISTRY AND P-T CONDITIONS.

EL-DESOKY, H.M.* and KHALIL, A.E.**

* *Department of Geology, Faculty of Science, Al-Azhar University.*
** *Department of Geology, National Research Center.*

Email hatem_eldesoky2002@yahoo.com

Abstract

Umm Rilan area is made up of talc-carbonate and talc serpentinite rocks of ophiolitic mélange, metavolcanics and granitoid rocks. The derivatives of ultramafic rocks as a result of metamorphism and the neighboring massive metavolcanic of the Late Proterozoic orogeny are related to a dismembered Pan-African ophiolitic mélange. In ultramafic rocks talc occurs as lenticular veins and along shear zone planes. Talc-carbonate rocks are whitish green, massive, slightly deformed, very fine- to fine-grained and composed of talc with carbonates as well as iron and manganese oxides as accessories. The talc carbonate rocks consist essentially of talc, malachite, dolomite, tremolite and magnesite. Geochemically, these rocks exhibit mafic-ultramafic cumulate ophiolite rocks of metamorphic peridotite and dunite in composition. The different variation diagrams indicate that these rocks are originated from cumulative komatiite with tendency to be tholeiitic magma and revealed that these rocks are formed in low Ti-ophiolites of tholeiitic environment. The scanning electron microscopic analysis detected that, the presence of Ta, Zn and Fe minerals in association with Cu, Ca and Mg mineralization. The contents of Cu, Zn and Pb show high tendency to be concentrated in the hydrothermally altered products associated with the sulfide minerals. The studied talc-carbonate rocks suffered low grade metamorphism in greenschist facies and was formed under medium pressure and low temperature of low Al_2O_3/CaO ratio related to the ultramafic rocks. Umm Rilan talc-carbonates are of hydrothermal origin. Tectonic activity plays a major role in the formation of Umm Rilan talc deposits by allowing fluids to penetrate the ultramafic rocks, creating a micro-permeability that facilitates reactions with the host rock (ultramafic-mafic rocks).

Key words: talc-carbonates, ultramafic-mafic rocks, ophiolite, petrography, geochemistry and metamorphism.

1. Introduction

Talc is a common metamorphic mineral occurs in metamorphic belts which derived from ultramafic rocks, such as soapstone (a high-talc rock) and within metavolcanics and blueschist metamorphic terranes (**Deer et al., 1992**).

The present work deals with field geology, petrography, geochemistry and metamorphic conditions of talc-carbonate rocks and talc mineralization in Wadi Umm Rilan area. Umm Rilan area is situated in north and south of central Wadi

Allaqi and located at 210 km southeast Aswan. This area is located between Latitudes 22°26′ – 22°29′ N and Longitudes 33°32′ - 33°37′ E (Fig.1).

The majority of talc occurrences in Egypt are derived from or hosted within the ultramafic rocks, mainly by serpentinite and mafic rocks as highly sheared metabasalts. Serpentinite bodies characteristically occur in belts of low-grade metamorphic rock. These talc deposits are widely variable in shape, and are mostly shear pods in shape, lenticular, thin shells and irregular masses.

This association of rocks characteristically consists of a talc core, surrounded by a shell of talc-carbonate in association with highly sheared serpentinite rock. The adjacent country rocks are altered to chlorite and biotite minerals at the contact between the talc-serpentinite and granitic rocks. Talc occurs as a secondary mineral formed by alteration of magnesium carbonates (magnesite and dolomite) and magnesium and/or iron silicates such as serpentine.

Salem (1992) recognized two distinct types of ultramafic-derived talc ore; pure talc and chlorite-talc. He also proposed that the talc deposits hosted by ultrabasic rocks were formed through processes of regional metamorphism and thrust faulting of serpentinized ultramafics and followed by percolation of hydrothermal solutions.

Rashwan et al. (1995) concluded that Umm Rilan area has been affected by four phases of deformation (D_1-D_4) within Pan-African orogenesis and D_5 strike-slip faults probably later than the Pan-African events. Allaqi shear zone separates the major lithostructural units.

The other type of talc deposits in Egypt occurs within a metavolcanic suite of tholeiitic affinity and Early Precambrian age (comprising metabasalt and metavolcanoclastic equivalents). These rocks have been transformed by successive phases of metasomatism into amphibolititized, chloritized, talc and talc-carbonate rocks. These talc deposits have been attributed to the flow of hydrothermal solutions rich in Si, CO_2, Fe and S along tectonized shear zones **(Said 1962; Hassan 1969)**. **Abdel Kader and Shalaby (1982)** studied the alteration zones at the Atshan talc mine and recognized three stages of alteration; serpentinization and carbonatization, sericitization or argillization and talcification.

Hussein (1990) proposed that the talc deposits hosted by metavolcanic rocks in Egypt were formed through a process of intense Mg-metasomatism associated with a volcanic exhalative episode. This exhalative episode was responsible for the formation of the massive Zn±Cu±Pb deposits, with which the talc has a close spatial association.

Nasr and Masoud (1999) concluded that the intensive Mg metasomatism took place along NW – SE shear zones produced talc lenses or pockets enclosed within these shear zones.

2. Analytical procedures

The mineralogical composition of talc-carbonate and the country rocks were confirmed by both X-ray difraction (XRD) and scanning electron microscope (SEM) techniques. Quantitative analyses were performed on talc, malachite, goethite and ferrite using a SEM with (EDS Link AN 10000 System). These analyses were carried out at the National Research Center (NRC), Dokki, Egypt. The analyses for total iron and Fe^{2+} were carried out by titration against $KMnO_4$ separately, thus Fe^{3+} is obtained by calculations.

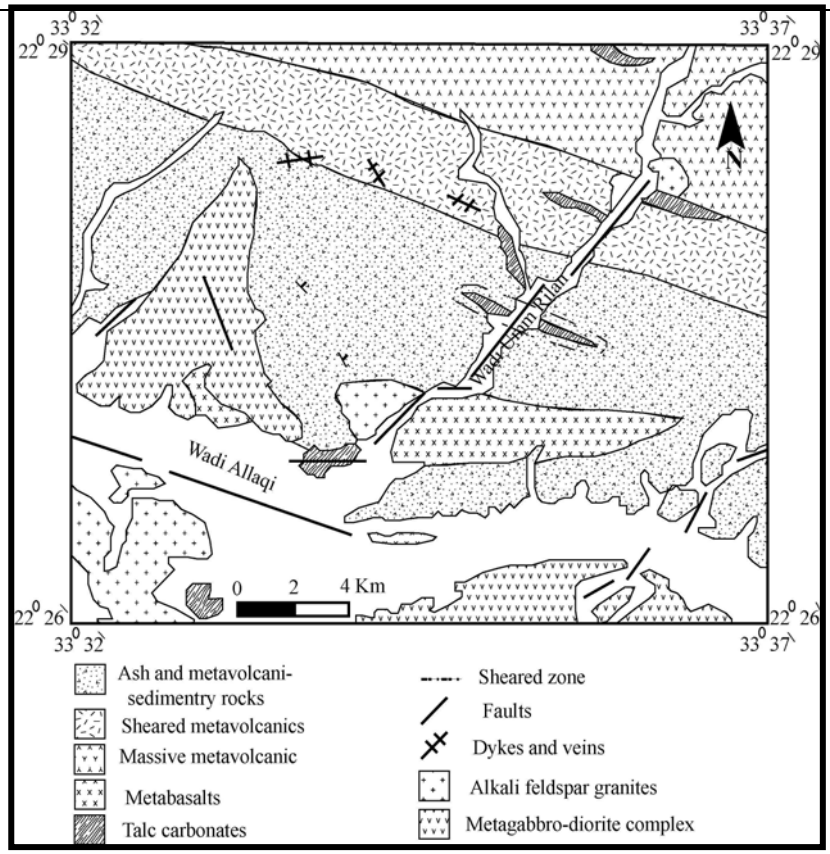

Fig.1: Geologic map of Wadi Umm Rilan area (After El-Kazzaz, 1995).

3. Field description

Umm Rilan area is of low to moderate relief, made up of two suites, metamorphic talc-carbonate and talc serpentinite rocks of ophiolitic mélange (Figs. 2 & 3), metavocanics (metabasalts) and granitoid rocks.

Talc-carbonate rocks are whitish green, massive, slightly deformed and very fine- to fine-grained and composed of talc with carbonates and iron and manganese oxides as accessories (Fig. 4). These talc-carbonate rocks occur as slices, heavily altered and are now represented by talc rocks and relics of serpentinites. Seven main talc lenses associated the talc serpentinite rocks in the studied area.

These talc-carbonate rocks contain euhedral cubes of goethite pseudomorphs most probably after pyrite or hematite (Figs. 5, 6 & 7); these cubes of goethite are well-developed and showing colloform texture. Low-temperature hydrothermal deposits of alkali feldspar granites yield pyrite as a primary mineral in granite and goethite as the hydrothermal alteration product of primary Fe-sulfides.

Talc is considered of a very good quality. It is pure white, massive and occasionally stained by malachite and manganese dendrite shape along fractures and joints as impurities (Fig. 8). The talc lenses and pockets reach up to 65 m in length and ranges from 25 to 30 m in width. They show preferred orientation where they fall within a plane striking from 110° to 130° and dipping from 50° to 60° NE.

The talc lenses occur along the shear zone in the mafic and ultramafic rocks which were affected by hydrothermal solutions rich in magnesium. These talc lenses are present as undulating boudinaged structures within the serpentinites and metabasalts (Fig. 9).

Umm Rilan alkali feldspar granite is a homogenous oval-shaped of about 1/2 Km^2 area (Fig. 10). It intrudes the talc-carbonate and talc serpentinite rocks with clear intrusive contacts as well as intercalations along a prominent shear zones. This granite is well jointed and sigmoidally sheared muscovite-bearing granite.

Fig.2: Photograph showing talc-carbonate lens within the metavolcanics.

Fig.3: Photograph showing talc serpentinite rocks of ophiolitic mélange.

Fig.4: Photograph showing the talc-carbonate rocks.

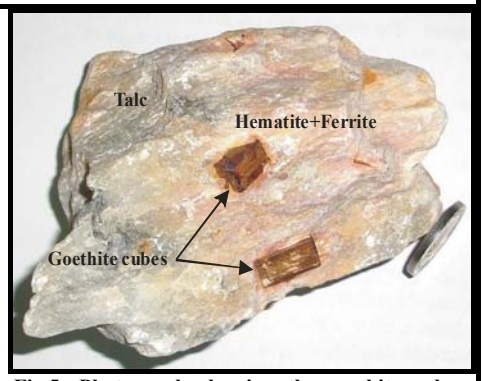

Fig.5: Photograph showing the goethite cubes after pyrite within the talc-carbonate rocks.

Fig.6: Photograph showing the goethite cubes.

Fig.7: Photograph showing talc stained by hematite after pyrite.

The southern margin of the body is affected by strong shearing, which has obliterated any evidence for intrusion and individual shears can be traced into the granite body. **El-Kazzaz (1995)** mentioned that, the muscovite commonly develops in rocks found in shear zones during the decompression stage following high strain. In the case of Umm Rilan granite this could be as late as the period following the D_2 phase of deformation.

4. Petrography and X-ray diffraction analysis

Talc-carbonate rocks consist essentially of talc, malachite, dolomite and magnesite. Goethite, tremolite and antigorite are the main secondary minerals. Iron oxides, gismondite and manganese oxides are the main accessories.

Talc is the most abundant mineral constituent that forms more than 90% of the rock volume. It occurs in coarse to fine platy or fibrous aggregates that often have a more or less parallel arrangement (Fig. 11). It is also found as shreds and plates that often bent. Two generations of talc are identified; the first occurs in the form of fine shreds less than 0.1 mm which show different orientation and sometimes show slight parallel arrangement forming schistose-like texture (Fig. 12). The second is medium to coarse plates up to 2mm are found by the talcification of olivine and pyroxene minerals. These plates have straight extinction, sometimes mottled, perfect cleavage and 3rd order of interference colors (Fig. 11).

The carbonate minerals occur in different forms such as malachite, dolomite and magnesite carbonate veinlets and as carbonate patches.

Malachite occurs in fine to coarse aggregates, usually xenomorphic and pale green, but it is often cloudy (Fig. 13). Malachite also occurs as pseudomorph after chalcopyrite and native copper. It is a common alteration product of copper minerals, resulting from the action of carbonated waters and hence is found in smaller or larger quantities in the upper levels of Umm Rilan copper mine. Malachite masses may contain the iron oxides and manganese ores.

Fig.8: Photograph showing talc stained by malachite and manganese.

Fig.9: Photograph showing talc present as undulating boudinaged structures.

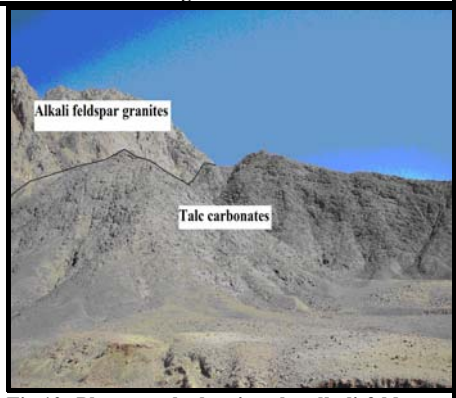

Fig.10: Photograph showing the alkali feldspar granites. 250 mμ

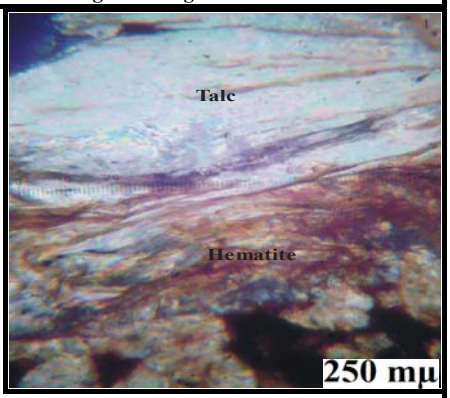

Fig.11: Photomicrograph showing talc fibrous aggregates showing parallel arrangement (CN).

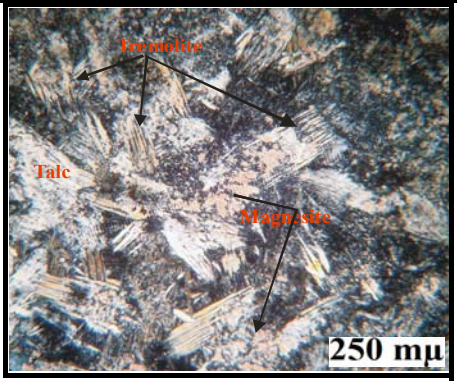

Fig.12: Photomicrograph showing talc as fine shreds of different orientation and fine-grained tremolite (CN).

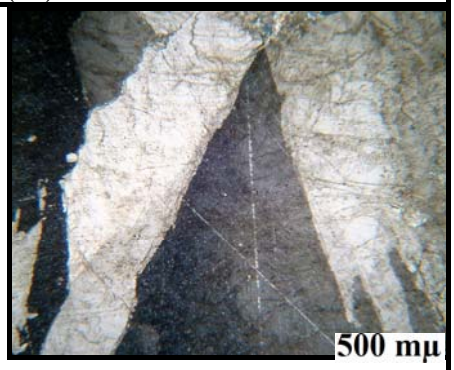

Fig.13: Photomicrograph showing malachite coarse aggregates (CN).

Dolomite occurs as fine- to coarse-grained and usually subidiomorphic. Zonal structure is frequent (Fig. 14); it is caused by variation in iron content. Dolomite xenocrystals show wavy extinction. **Magnesite** usually occurs in xenomorphic to subidiomorphic crystal aggregates and colorless to pale grey and found as veins (Fig. 15) in talcose serpentinite rocks. Magnesite within talc-carbonate rocks is commonly the result of the hydration and carbonation of magnesium minerals (olivine) found in ultramafic rocks. **Antigorite** occurs as a secondary mineral after the antigoritization of the original ultramafic minerals (Fig. 16). Antigorite is colorless to pale green, tiny flakes, shreds, fibers and lamellae. It also occurs in subidiomorphic crystal aggregates of fibro-lamellar structure. **Tremolite** occurs as an alteration products; colorless to pale brown in color. The brown varieties show faint pleochroism and occur in columnar to fibrous aggregates (Fig. 12). Tremolite rich bearing rocks are altered along shear zone to talc carbonate rock.

Umm Rilan alkali feldspar granites are mainly consist of quartz, plagioclase and alkali feldspar with muscovite, sphene and iron oxides as accessory minerals. Kaolinite is present as secondary minerals. They are coarse-grained and form hypidiomorphic texture.

Quartz forms clear colorless and anhedral to subhedral intergranular grains which may show undulatory extinction (Fig. 17). The feldspars are represented by plagioclase and microcline. **The plagioclase** feldspar is commonly zoned albite and forms megacrysts in the porphyritic variety and usually occurs as euhedral to subhedral elongate crystals (Fig. 18). **Alkali feldspar** is represented mostly by unzoned microcline which forms tabular subhedral to anhedral and may occur as phenocrysts. **Sphene** is found as small crystals of irregular shape (Fig. 19). It is usually associated with black iron oxides (Fig. 19). **Iron oxides** occur either as euhedral fine crystals or as fine disseminated grains. **Muscovite** is present as fine flakes, subhedral to anhedral crystals and fracture-filling mineral in the form of stretched flow banding due to deformation (Fig. 17) and is mainly altered to sericite. Kaolinite is an alteration product after microcline.

X-ray diffraction analysis results

Eight samples from talc-carbonate deposits have been subjected to X-ray diffraction analysis. They reveal that the talc carbonate rocks are composed of talc, dolomite, magnesite, gismondite and antigorite (Figs. 20, 21 & 22) confirming the

results of the microscopic investigations. XRD for one cube enclosed within the talc show that these cubes are goethite mineral (Fig. 22).

5. Geochemistry of the talc-carbonate rocks

Representative samples were collected from the talc serpentinite and talc-carbonate deposits. Two pure talc and seven talc carbonate rock samples were chemically analyzed for major oxides and trace elements using XRF technique (Table 1).

The talc-carbonate rocks are represented by talc-malachite-antigorite-Mn ore, talc-goethite, talc-dolomite-antigorite-Fe ore, talc-dolomite-magnesite-antigorite, talc-dolomite, talc-dolomite-malachite-antigorite, talc-dolomite-antigorite and talc-malachite.

Chemical distribution of the talc carbonates.

As shown in table (1) representing its chemical analyses, the investigated talc-carbonate rocks have wide range of the chemical composition chiefly SiO_2, MgO and CaO. The low Al_2O_3, Fe_2O_3 and FeO contents are combined with high MgO to give composition of antigorite with talc. Tremolites associated with talc show much lower values of Al_2O_3 and relatively Fe_2O_3 with higher CaO content. Talc also associated with small amounts of dolomite (sample 5) shows high CaO content.

In the talc-carbonate rocks SiO_2 ranges from 9.01% to 60.79%, MgO from 21.37% to 36.80%, Al_2O_3 from 0.16% to 2.49% and CaO from 0.02% to 26.80%. Na_2O, K_2O and P_2O_5 are extremely low and L.O.I. is high (0.40%-41.07%). These rocks show a limited range of FeO (0.018-1.63%), Fe_2O_3 (0.02-1.86%) and MnO (0.01-0.12%).

The chemical analyses of the talc-carbonate samples show high concentration of Ni reaching 1800 ppm and Cr up to 2100 ppm, which is probably attributed to the enrichment of amphibole or pyroxene minerals in Ni and Cr. Compared with talcified rock carbonatized at Darhib area, South Eastern Desert, Egypt (**Salem et al., 1999**), Sr content is rather close, Zr is higher, while Cu is relatively higher, this due to the enrichment of malachite mineral. Copper is associated with malachite, which formed as a result of the leaching of primary sulfide minerals, where considerable number of samples are observed stained by malachite (Fig.8).

Table 1. Major oxides and trace elements of Umm Rilan talc-carbonate rocks.

Sample No.	1	2	3	4	5	6	7	8	9	TC
Major oxides (Wt. %)										
SiO_2	45.60	60.79	40.46	23.37	9.01	60.70	31.58	34.81	43.62	30.79
TiO_2	0.01	0.01	0.01	0.01	0.01	0.04	0.01	0.01	0.01	--
Al_2O_3	2.49	0.65	0.59	0.16	1.04	0.20	0.38	2.17	0.68	0.15
FeO	0.09	1.63	0.43	0.018	0.14	1.48	0.13	0.20	0.31	--
Fe_2O_3	0.10	1.86	0.48	0.02	0.16	1.65	0.14	0.22	0.34	0.53
MnO	0.01	0.02	0.12	0.02	0.01	0.01	0.48	0.03	0.05	0.26
MgO	36.80	30.42	26.86	30.03	21.37	30.67	28.11	32.89	35.11	25.78
CaO	0.46	0.02	9.98	8.46	26.80	0.26	12.56	6.54	0.75	15.29
Na_2O	0.02	3.10	0.03	0.01	0.02	3.18	0.01	0.03	0.02	--
K_2O	0.01	1.50	0.01	0.01	0.01	1.57	0.01	0.01	0.01	0.02
P_2O_5	0.31	0.01	0.05	0.05	0.01	0.01	0.42	0.11	0.10	0.04
LOI	12.36	0.88	21.07	37.72	41.07	0.40	26.26	21.23	18.26	26.90
Total	98.16	99.25	99.64	99.85	99.48	99.98	99.92	98.04	98.93	99.76
Trace elements (ppm)										
Sr	8	11	59	15	16	12	83	30	41	52
Zr	30	341	28	10	27	345	25	21	23	3
Nb	3	2	3	9	2	3	2	4	3	1
Pb	32	7	30	11	57	8	20	33	23	10
Zn	61	160	87	17	86	161	158	175	143	120
Cu	34	25	9	32	39	24	67	35	65	10
Ni	1300	1400	1345	1200	1200	1400	1562	1600	1800	--
V	13	18	18	15	25	20	27	25	23	<1
Cr	1540	2101	2145	1800	2154	2106	1789	1650	1640	--
Co	77	88	80	45	2	85	78	65	55	1
As	0.3	4	2	5	8	4	3	5	7	--

TC: Talcified rock carbonatized at Darhib area, Eastern Desert, Egypt (Salem et al., 1999).
1-Talc-malachite-antigorite-Mn ore. 2-Talc-goethite.
3-Talc-dolomite-antigorite-Fe oxides. 4-Talc-dolomite-magnesite-antigorite.
5-Talc-dolomite. 6-Talc-goethite.
7-Talc-dolomite-malachite-antigorite. 8-Talc-dolomite-antigorite. 9-Talc-malachite.

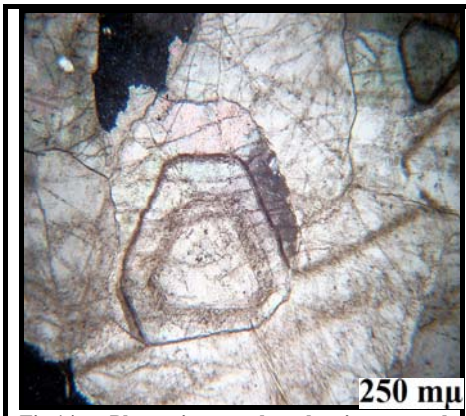

Fig.14: Photomicrograph showing zonal structure within dolomite (PPL).

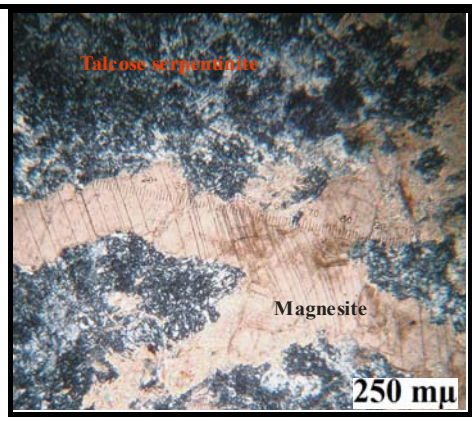

Fig.15: Photomicrograph showing magnesite veins within talcose serpentinite (CN).

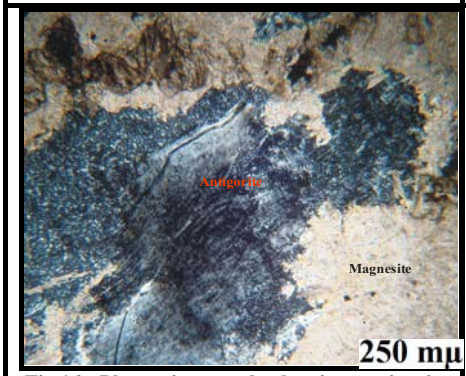

Fig.16: Photomicrograph showing antigorite and magnesite crystals (CN).

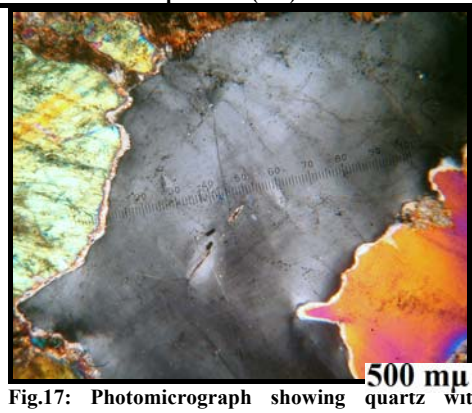

Fig.17: Photomicrograph showing quartz with undulatory extinction and muscovite high order of interference colors (CN).

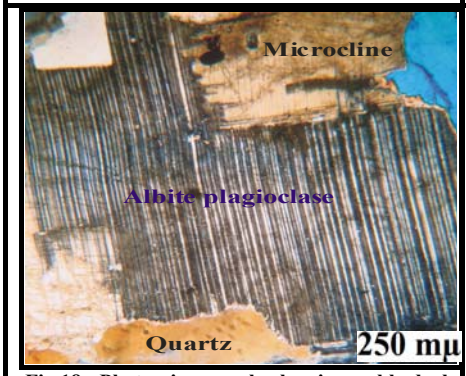

Fig.18: Photomicrograph showing subhedral elongated plagioclase crystals (CN).

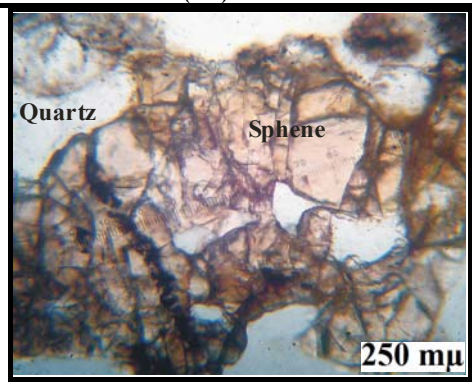

Fig.19: Photomicrograph showing brown sphene irregular shape with black iron oxides (PPL).

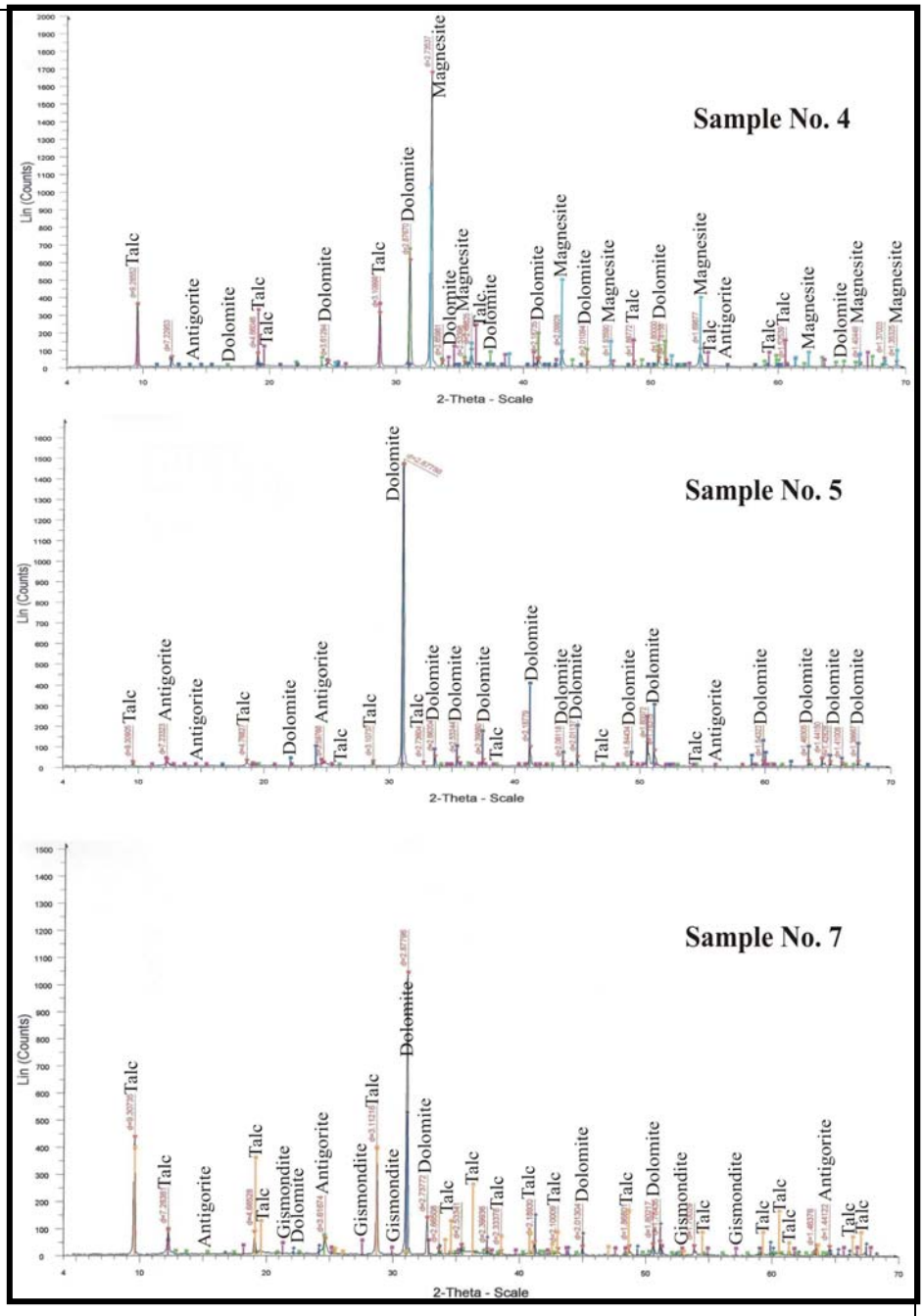

Fig.21: X-ray diffraction patterns showing the talc-carbonate minerals.

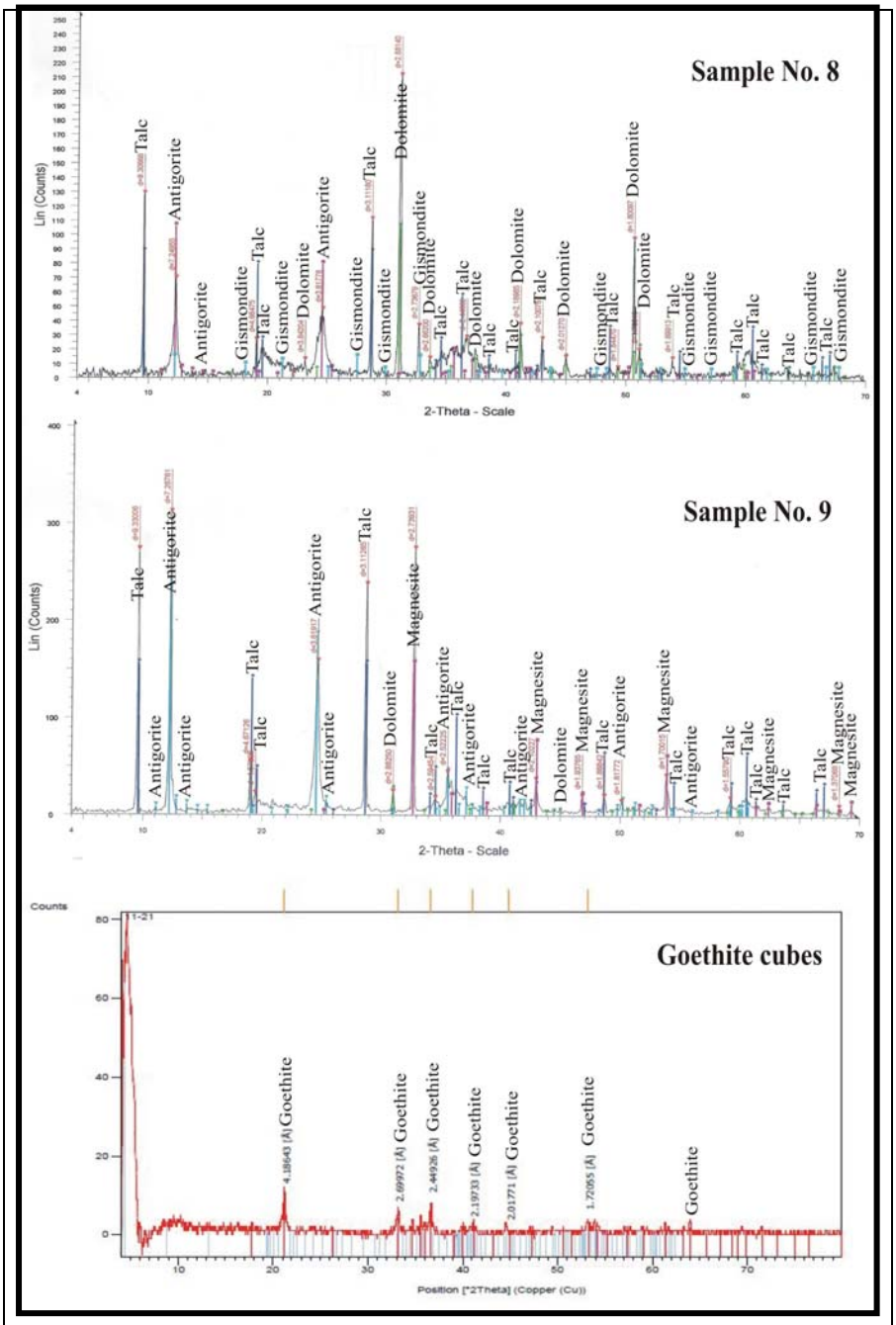

Fig.22: X-ray diffraction patterns showing the talc-carbonate minerals and goethite mineral.

The contents of Cu, Zn and Pb show high tendency to be concentrated in the hydrothermally altered products (slightly talcified, serpentinized, carbonitized and slightly altered metavolcanic rocks) associated with the sulfide minerals. Pb is found in small amounts this reflects that pyrite in oxidized zone altered to goethite, ferrite and hematite.

The relatively high contents of V and Co and the low contents of Nb and As confirm that the studied talc carbonate rocks are originated from ultrabasic parental rocks.

The **Niggli (1954)** values for the talc-carbonate rocks were listed in Table 2 and show the following characteristics:-

1. Low alk, k, mg and high fm values which is consistent with its ultramafic-mafic nature and mineralogical composition.

2. The heterogeneous character of the talc-carbonate rocks.

3. The **al** in the talc carbonate rocks does not show any definite trend and exhibit low values except three samples (1, 6 and 8).

4. The presence of **c** in all samples reflects the hydrothermal nature of these rocks especially samples 3, 4, 5 and 7.

5. The **k** and **alk** in these rocks are very low contents except two samples (2 and 6) which were derived from hydrothermal nature.

The calculated mesonorm (**Barth, 1962**) values listed in Table 3 are characterized by the following:-

1. High values of normative hypersthene (6.18-72.70%), olivine (39.31-73.69%), diopside (1.10-91.14%) and enstatite (6.16-61.82%).

2. Normative biotite, actinolite and riebeckite are recorded in few samples of talc goethite rocks. The chemical composition of these samples showed that they are rich in Na_2O, MgO and Fe_2O_3 relative to the other samples of the talc-carbonates.

3. Normative spinel and corundum exist in two samples (1 and 8) revealing its high temperature metamorphic nature of forsterite and diopside.

4. Fair percentages of normative ferrosilite, sphene, magnetite and apatite are recorded in all samples.

5. Very low normative albite and anorthite in some samples.

6. The presence of normative Wo in one sample (9) of talc malachite rocks instead of hypersthene. Regarding the mesonorm calculations wollastonite calculated instead of hypersthene and vice versa; thus, the two normative minerals are not recorded in one sample.

5- The presence of normative quartz, sodium metasilicate and potassium metasilicate in two samples (2 and 6) of talc goethite rocks this is due pneumatolytic metamorphism. In addition much quartz is developed by the release of SiO_2 in reactions taking place during hydrothermal metamorphism.

From the above mentioned Niggli values and mesonorm composition, these rocks were subjected to thermal and regional metamorphism of the low grade metamorphism in the greenschist facies supported by presence of secondary chlorite, epidote, tremolite, actinolite and carbonate (magnesite and calcite).

There are different types of talc are represented by pure talc, talc-carbonate and talc serpentine are while the slightly talcified rocks are also represented by antigoritized, actinolitized and tremolitized rocks.

It is proposed that the high content of SiO_2 (samples 2 and 6) in the hydrothermal solution is due to alteration in the entire serpentinized body to talc.

Table 2. Niggli values of the Umm Rilan talc-carbonate rocks.

Sample No.	**1**	**2**	**3**	**4**	**5**	**6**	**7**	**8**	**9**
si	80.054	115.78	77.95	43.32	14.67	121.95	56.22	60.36	80.63
al	2.57	0.72	0.66	0.17	0.99	2.60	0.39	2.21	0.73
fm	95.56	91.69	78.68	83.01	52.23	85.20	75.65	85.59	97.73
mg	0.998	0.965	0.987	0.999	0.996	0.966	0.988	0.996	0.994
c	0.86	0.04	20.59	16.80	46.74	2.71	23.95	12.14	1.48
alk	0.033	7.54	0.05	0.017	0.03	9.48	0.001	0.04	0.04
k	0.001	0.24	0.001	0.001	0.001	0.35	0.001	0.001	0.238
si*	100.13	132.32	100.2	100.068	100.12	145.72	101.17	106.79	100.16
qz	-20.08	-16.54	-22.25	-65.75	-85.45	-95.05	-44.95	-46.43	-19.53

Table 3. Mesonorm values of the Umm Rilan talc-carbonate rocks.

Sample No.	1	2	3	4	5	6	7	8	9
Otz	--	6.65	--	--	--	7.17	--	--	--
Fs	0.04	--	0.29	0.03	0.02	--	0.36	0.08	0.16
Ks	--	1.46	--	--	--	0.92	--	--	--
Ns	--	6.10	--	--	--	6.73	--	--	--
Ab	0.05	--	0.16	0.08	0.14	--	--	0.1	0.06
An	0.08	--	0.87	0.36	2.40	--	0.61	--	0.77
Sp	21.85	--	--	--	--	--	--	19.53	--
Act	--	0.08	--	--	--	7.62	--	--	--
Tn	0.007	0.02	--	--	0.02	0.46	--	7.05	0.008
Mt	0.03	--	0.26	0.017	0.12	--	0.07	0.07	0.14
Ap	0.21	--	0.06	0.09	--	0.02	0.88	0.07	0.08
Hy	33.38	72.70	33.34	61.85	6.18	51.30	32.65	32.02	--
Bi	--	5.20	--	--	--	18.41	--	--	0.03
Ri	--	7.80	--	--	--	7.37	--	--	--
Wo	--	--	--	--	--	--	--	--	0.54
C	0.85	--	--	--	--	--	--	0.82	--
Ol	43.54	--	42.42	73.69	--	--	39.31	40.34	54.97
Di	--	--	22.88	30.74	91.14	--	26.47	--	1.10
En	33.34	--	33.05	61.82	6.16	--	32.30	31.94	42.14

The mineral reactions include alteration of olivine to serpentine, serpentine to talc and talc-carbonate, alteration of tremolite to chlorite and talc and alteration of chlorite to talc.

Chemical classification and nomenclature

For the classification and nomenclature of the talc-carbonate rocks the following elementary calculations and variation diagrams are used.

On the Al_2O_3-CaO-MgO ternary diagram of **Coleman (1977,** Fig.23), the samples plot within the fields of ultramafic rocks and metamorphic peridotite associated with ophiolites.

The SiO_2 - ($CaO+Na_2O+K_2O$) - (FeO*+MgO+MnO), ternary diagram of **Raymond, (1995)** shows that the data points fall in and nearby the fields of basic (B) and ultrabasic (U) rocks except one sample of talc-dolomite rock plots in carbonate and nonsilicate rocks (C) field (Fig.24). This is due to the high percentage of CaO and MgO confirming its talc-dolomitic rocks.

The plots of the samples on the (SiO_2-FeO*-MgO) ternary diagram of **Pfeifer (1979)**, fall within the dunite field (Fig.25).

On the AFM diagram (Fig.26) of **Coleman** (**1977**), the plotted samples fall in the fields of metamorphic peridotite and mafic-ultramafic cumulate ophiolite rocks.

On ACF diagram (Fig.27) of **Winkler** (**1976),** most data points plot close to the field of ultrabasic rocks (1), however, one sample falls towards the CF side. Meanwhile, on **Winkler** (**1976**) ACF diagram (Fig.28), the data points plot in and nearby the field of ultrabasic rocks.

The (SiO_2)-(H_2O)-(MgO) ternary diagram is proposed by **Bowen & Tuttle, (1949)** to discriminate the examined samples as derived from rocks of mafic-ultramafic cumulate (Fig.29). The analyzed samples plot in the talc-serpentine-olivine field and the plotted talc samples (2 & 6) lie near the talc point in the field of talc-SiO_2-orthopyroxene.

These are a series of discrimination diagrams developed by Archean geologists **(Hallberg, 1985)** for the discrimination and classification of altered ancient volcanic rocks as reproduced by **Rock, (1990)**.

According to **Rock, (1990)** the diagrams (Figs. 30 & 31) are suitable for ancient mafic ultramafic rocks in greenstone belts and probably certain other geological settings as in Umm Rilan area. The plots of samples on the (Cr)-(TiO_2) binary diagram fall within cumulative komatiites (CK) field (Fig. 30) enhancing ultramafic source rocks. In this respect, on the (Ni)-(Cr) binary diagram all samples occupy the fields of cumulative komatiites (CK) and layered high-Mg sills (LHM, Fig. 31).

Magma types of the talc-carbonate source rocks

The plotted samples on the AFM diagram of **Irvine and Baragar (1971)**, exhibit komatiitic affinity of the source rocks (Fig. 32). This is due to ophiolitic rocks.

The plots of the talc-carbonate samples on the various binary diagrams of K_2O-SiO_2 **Le Maitre (1989,** Fig. 33), Sr-Zr **Pearce (1975,** Fig. 34) and K_2O-SiO_2 **Miyashiro (1974,** Fig. 35) show that they are of low K-tholeiites magma type except two samples of talc-goethite (2 & 6).

In the K_2O-Na_2O binary diagram of **Mahnert (1968)**, the talc-carbonate rocks fall in the metamorphic basic field whereas the talc-goethite samples fall nearby the metamorphic acidic field (Fig.36).

Tectonic setting

On the TiO_2 versus (FeO*)/(FeO*+MgO) binary diagram (Fig.37) of **Serri** (**1981**), the plotted samples fall in the low Ti-ophiolite field supporting the ophiolitic origin of these rocks.

From the previously mentioned characteristics, the following features can be recorded:

1- The discrimination diagrams revealed that these rocks formed in low Ti-ophiolites.

2-The studied talc carbonate rocks exhibit mafic-ultramafic cumulate ophiolite rocks, metamorphic peridotite and dunite in composition. The different variations diagrams indicate that these rocks originated from cumulative komatiite magma.

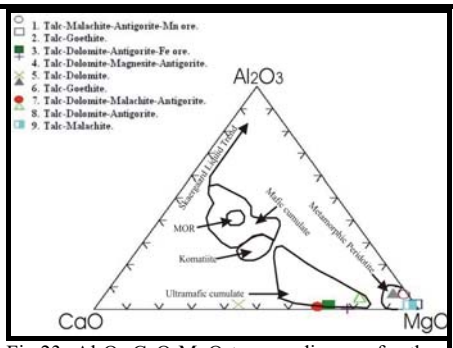

Fig.23: Al_2O_3-CaO-MgO ternary diagram for the talc-carbonates (**Coleman, 1977**).

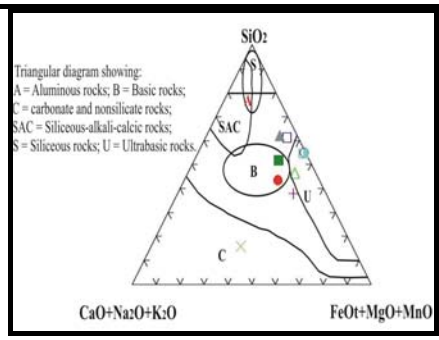

Fig.24: SiO_2-$CaO+Na_2O+K_2O$)-(FeO*+MgO+MnO) diagram for the talc-carbonates (**Raymond, 1995**). Legend as in Fig. (24).

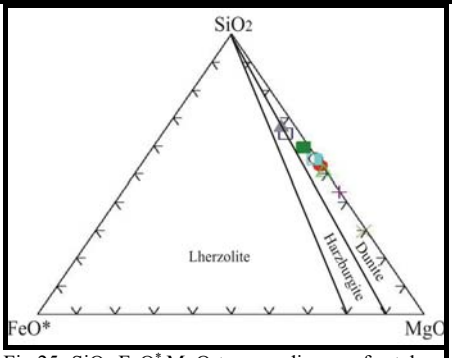

Fig.25: SiO_2-FeO^*-MgO ternary diagram for talc-carbonates (**Pfeifer, 1979**). Legend as in Fig. (24).

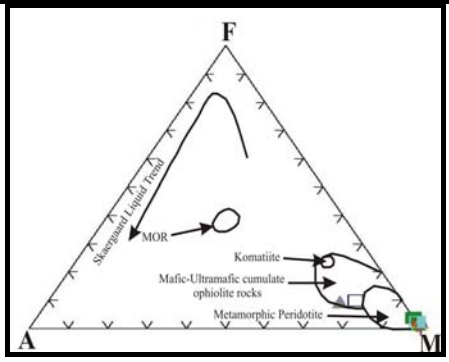

Fig.26: AFM ternary diagram for the talc-carbonates (**Coleman, 1977**). Legend as in Fig. (24).

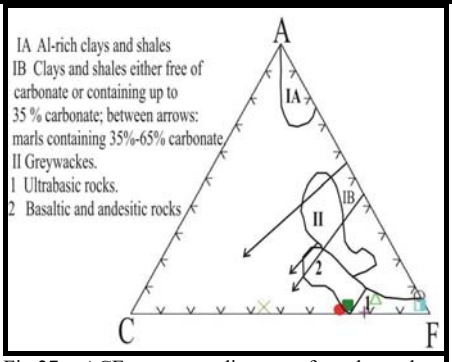

Fig.27: ACF ternary diagram for the talc-carbonates (**Winkler, 1976**). Legend as in Fig. (24).

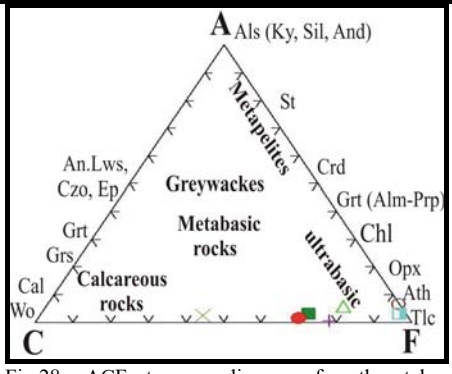

Fig.28: ACF ternary diagram for the talc-carbonates (**Winkler, 1976**). Legend as in Fig. (24).

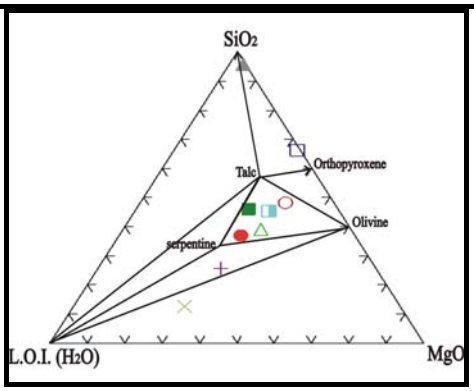

Fig.29: SiO_2-MgO-H_2O ternary diagram for talc-carbonates (Bowen & Tuttle, 1949). Legend as in Fig. (24).

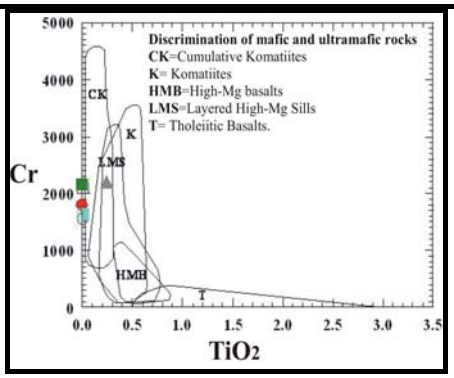

Fig.30: Cr versus TiO_2 discrimination binary diagram for the talc-carbonates (Rock, 1990). Legend as in Fig. (24).

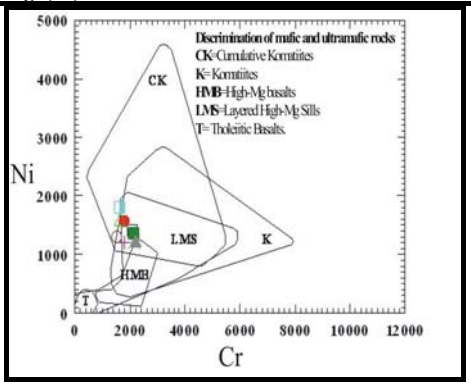

Fig.31: Ni versus Cr discrimination binary diagram for the talc-carbonates (Rock, 1990). Legend as in Fig. (24).

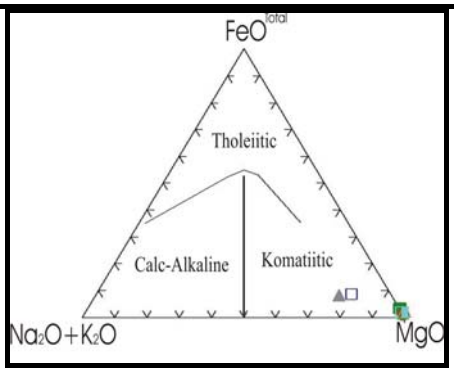

Fig.32: FeOt- (Na_2O+K_2O)-MgO ternary diagram for the talc-carbonates (Irvine & Baragar, 1971). Legend as in Fig. (24).

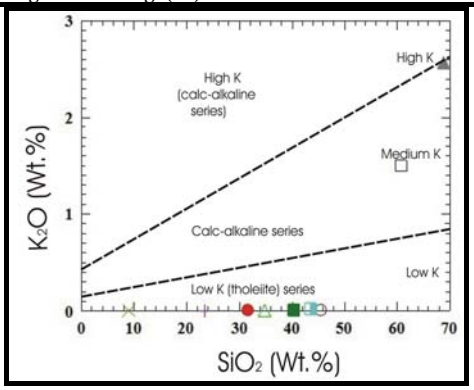

Fig.33: K_2O-SiO_2 binary diagram for the talc-carbonates (Le Maitre, 1989). Legend as in Fig. (24).

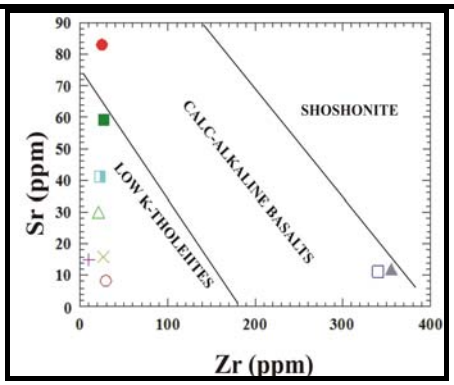

Fig.34: Sr versus Zr variation diagram for the talc-carbonates (Pearce, 1975). Legend as in Fig. (24).

Chemo-metamorphic characterizations

On the Al^{iv}- Si^{iv} variation diagram (Fig.38) of **Rasse** (**1974**), the majority of samples are encountered in low pressure field.

On the Ti and total Al binary diagram (Fig.39) of **Hynes** (**1982**), the samples except one (6) plot in the medium pressure amphibole field. This sample plot in the maximum of Ti for low pressure amphiboles.

The plotted samples on the CaO versus Al_2O_3 binary diagram (Fig.40) of **Aumento and Laubat (1971)** reveal that the majority of the samples fall within and nearby the oceanic low temperature of low Al_2O_3/CaO ratio values.

On the Na+K versus Ti binary diagram (Fig.41) of **Zakrutkin (1968)**, the analyzed samples are concentrated in greenschist facies field except a sample of talc-goethite rock (6) this due to its enrichment in secondary silica.

From all above relationships, it can be concluded that:-

1-The investigated talc-carbonate rocks are of low grade greenschist facies.

2-These rocks were formed under low to medium pressure / oceanic low temperature regional metamorphism of low Al_2O_3/CaO values causing limited variation in mineralogical and chemical compositions.

3-The abnormal position of the sample No.6 (talc-goethite rock) in these discrimination diagrams is due to its enrichment in secondary silica, iron oxides, alumina and alkalies and depletion in lime and titanium. The high values of SiO_2, Al_2O_3, (K_2O+Na_2O) and (FeO+Fe_2O_3) may be attributed to several alteration processes such as goethitization and kaolinitization affected the rock of this sample.

6. Scanning Electron Microscopic Study

The X-ray micro-analyses specially give both qualitative and quantitative information about the element composition of scanned minerals. The EDX qualitative micro-analyses identify the elements occurring in the analyzed specimens, whereas the quantitative microanalyses show how much of a particular element is present in the analyzed specimens.

The SEM estimation and the EDX spectra of the thin polished surface from the metamorphosed talc-carbonate are used to identify the mineral association in these

rocks. The X-ray spectra and tabulated data of quantitative EDX analysis indicate that most of ferrite crystals are hosted in the talc carbonate rocks.

Nine thin polished sections were studied under the scanning electron microscope to get more information about the talc carbonate minerals and their interrelationships. The results obtained show the following mineral association:-

1- Talc ($Mg_3 Si_4 O_{10} (OH)_2$). The talc deposits have inherited trace elements from the parent ultramafic rocks and contain trace elements from the hydrothermal solutions from alkali feldspar granites where the latter seem to have lower concentrations of these elements.

Talc is formed by the addition of SiO_2 and MgO and by remove Al_2O_3, CaO, Fe_2O_3 and Na_2O+K_2O of the mafic and ultramafic rocks.

2- Malachite ($Cu_2 CO_3 (OH)_2$) occurs as irregular patches disseminated in the talc serpentinite rock due to the alteration of Cu sulfides and stained the rock with green color. Malachite occurs also in highly sheared talcose rocks of shear zone. It is characterized by green color, strong pleochroism, low reflectance color and strong anisotropism but polarization is partially masked by abundant green internal reflection color. Malachite permeates the veinlets along the fractures, cracks and joints in the talc-carbonate rocks.

3- Ferrite ($ZnFe_{18}O_{27}$) shows white or grayish white color, moderate reflectance color and weak anisotropy. It occurs as fine to medium broad shaped bodies scattered greatly within the talc-carbonate rocks. The hexagonal ferrites make up a large family of compounds with the general formula $mAO.nMeO.oFe_2O_3$, where A = Sr, Ba, or Pb and Me = Mg^{2+}, Mn^{2+}, Fe^{2+}, Co^{2+}, Zn^{2+}. The crystal structure systematics of the family was investigated first by **Braun (1957)**.

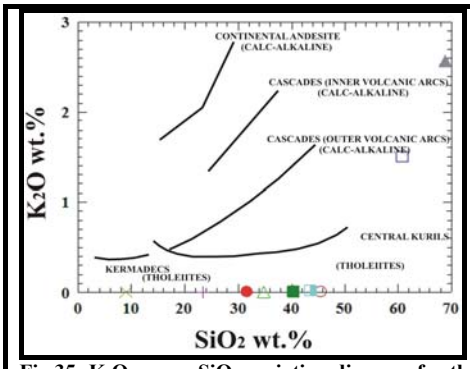

Fig.35: K_2O versus SiO_2 variation diagram for the talc-carbonates (Miyashiro, 1974). Legend as in Fig. (24).

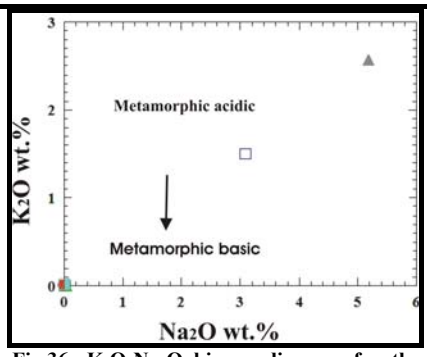

Fig.36: K_2O-Na_2O binary diagram for the talc-carbonates (Mehnert, 1968). Legend as in Fig. (24).

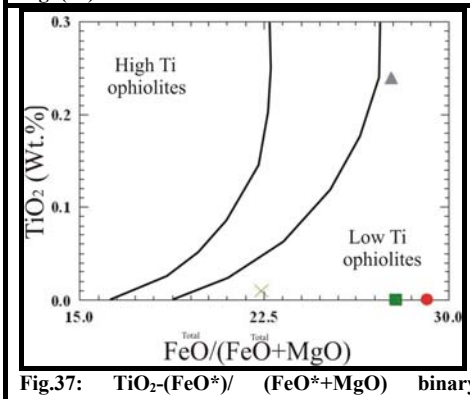

Fig.37: TiO_2-(FeO*)/ (FeO*+MgO) binary diagram for the talc-carbonates (Serri, 1981). Legend as in Fig. ().

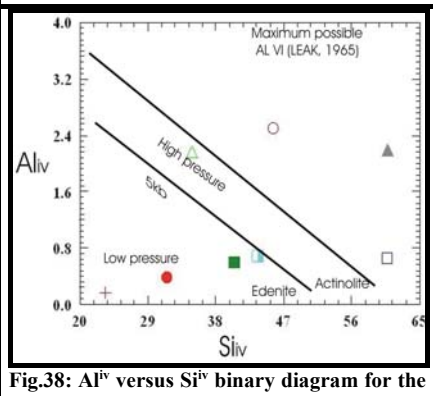

Fig.38: Al^{iv} versus Si^{iv} binary diagram for the talc-carbonates (Rasse, 1974). Legend as in Fig. (24).

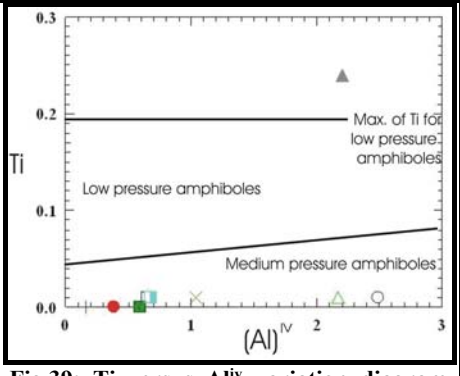

Fig.39: Ti versus Al^{iv} variation diagram for the talc-carbonates (Hynes, 1982). Legend as in Fig. (24).

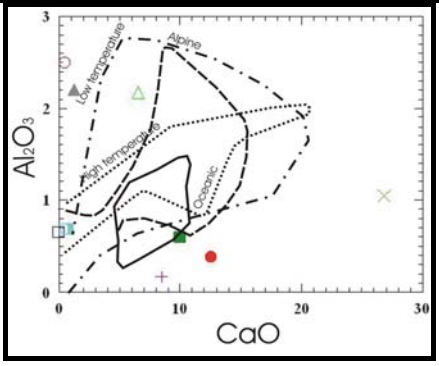

Fig.40: Al_2O_3-CaO binary diagram for the talc-carbonate (Aumento and Laubat, 1971). Legend as in Fig. (24).

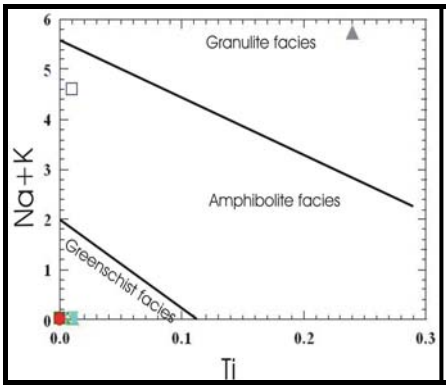

Fig.41: Na+K versus Ti binary diagram for the talc-carbonate (Zakrutkin, 1968). Legend as in Fig. (24).

Structurally they are known as the M-type ferrites. The present paper reports on a new Zn-bearing hexagonal ferrite mineral from the Umm Rilan talc deposit. Typically the ferrites have a banded appearance, with oxides and calcium and magnesium silicates concentrated in irregular layers, intercalated with parts rich in carbonates (Fig.42).

Also the scanning electron microscopic analysis detected presence of Ta, Zn and Fe minerals in association with Cu, Ca and Mg mineralization as shown in Figures (42, 43 & 44).

The results of this study show that, the recorded Ta, Zn and Cu mineralization at the contacts between talc-carbonate rocks and alkali feldspar granites as well as the wall rock alteration zones by leaching and redeposition during the deformation stages affected these rocks.

7. Evolution of metamorphic changes and hydrothermal conditions

Petrographical observations, petrochemical characterizations and chemo-metamorphic history lead to concordant result on the great proportions of talc (>80 wt. %) in these rocks. Talc-carbonate rocks within ophiolite complex in South Eastern Desert of Egypt, is best explained by a combination of regional metamorphism and hydrothermal or contact metamorphism associated with igneous activity at a spreading centre.

Talc occurs in talc-rich serpentinite or steatite through hydrothermal alteration of mafic rocks (steatitization) subsequent to serpentinization during greenschist facies metamorphism. Talc also formed by thermal low-temperature metamorphism of

siliceous dolostones. The mineral associations are antigorite, magnesite, dolomite and calcite.

Generally, in retrograde or low-grade metamorphism, talc is a minor phase among many assemblages (**Müller et al., 2003**). For an important deposit displaying such high talc content, a hydrothermal origin is favored. Coexisting calcic amphiboles strengthen the hydrothermal origin.

Another important result deduced from chemical data is the ultrabasic and basic nature of the original rocks. Successive metamorphic and hydrothermal reactions have replaced or dissolved all primary minerals which were likely olivine and pyroxenes.

Basically, some possible reactions for talc and tremolite crystallization subsequent to olivine and pyroxene replacement are:-

$2Mg_2SiO_4+3H_2O \leftrightarrow Mg_3Si_2O_5(OH)_4+Mg(OH)_2$ (**Deer et al., 1992**)

Forsterite water serpentine brucite

$2CaMgSi_2O_6+3Mg_2Si_2O_6+3H_2O \leftrightarrow$

Diopside enstatite water

$Ca_2Mg_5Si_8O_{22}(OH)_2+Mg_3Si_2O_5(OH)_4$) **Mével, 2003**)

tremolite serpentine

Fluid coming from the surrounding alkali feldspar granite may be rich in dissolved SiO_2.

$Mg_3Si_2O_5(OH)_4+2SiO_2 \leftrightarrow Mg_3Si_4O_{10}(OH)+2H_2O$

Serpentine fluid talc fluid

Talc crystallizes in a wide range of temperature. It cannot thus help to constraint temperature. Its formation is controlled by other factors, particularly silica activity in the fluid phase (**Mével, 2003**).

A most striking feature is the development of tremolite at the expense of talc. The reverse phenomenon is observed in the talc deposits in the Eastern Desert, Egypt (**Schandl et al., 2002**).

8. Talc Mineralization

Umm Rilan talc deposits are of hydrothermal origin. Tectonic activity plays a major role in the formation of Umm Rilan talc deposits by allowing fluids to penetrate rocks, creating a micro-permeability that facilitates reactions with the host rock. Umm Rilan talc deposits associated with mafic and ultramafic rocks. In ultramafic rocks talc commonly occurs as lenticular veins and along shear zone planes.

Talc can be formed during serpentinization of the ultramafic rocks usually peridotite. The process is followed by carbonatization during which fluids containing more than 5 % CO_2 are introduced and a talc-carbonate rock is formed. This rock may be further transformed into steatite through the interaction with silica-bearing solutions. The talc rock may replace lenses or large masses of serpentinite. The talc lenses may measure several hundred meters long by several hundred meters wide. These occurrences constitute the largest talc deposits but can contain more impurities, most notably asbestos minerals.

Talc-carbonate deposits associated with metavolacanic rocks are formed in the same way as those associated with serpentinite rocks. Talc can develop by serpentinization of mafic rocks like basalt. These deposits generally produce low quality soapstone and are rarely economical to exploit.

The rocks which host the talc deposits are metamorphosed mafic and ultramafic rocks. These rocks appear to have undergone regional metamorphism followed by hydrothermal alterations (chloritization, tremolitization and silicification). The mafic rocks are of tholeiitic nature and are interpreted to have erupted in a deep oceanic ridge.

Metasomatic changes associated with hydrothermal alteration are related to the emplacement of nearby younger alkali feldspar granitic intrusions of Umm Rilan. These include the formation of talc and minor quantities of carbonates. SiO_2, H_2O and CO_2 have been introduced to the system but all other constituents are inherited from the parent ultramafics. It is proposed that SiO_2 in the hydrothermal solution altered the entire serpentinized body to talc.

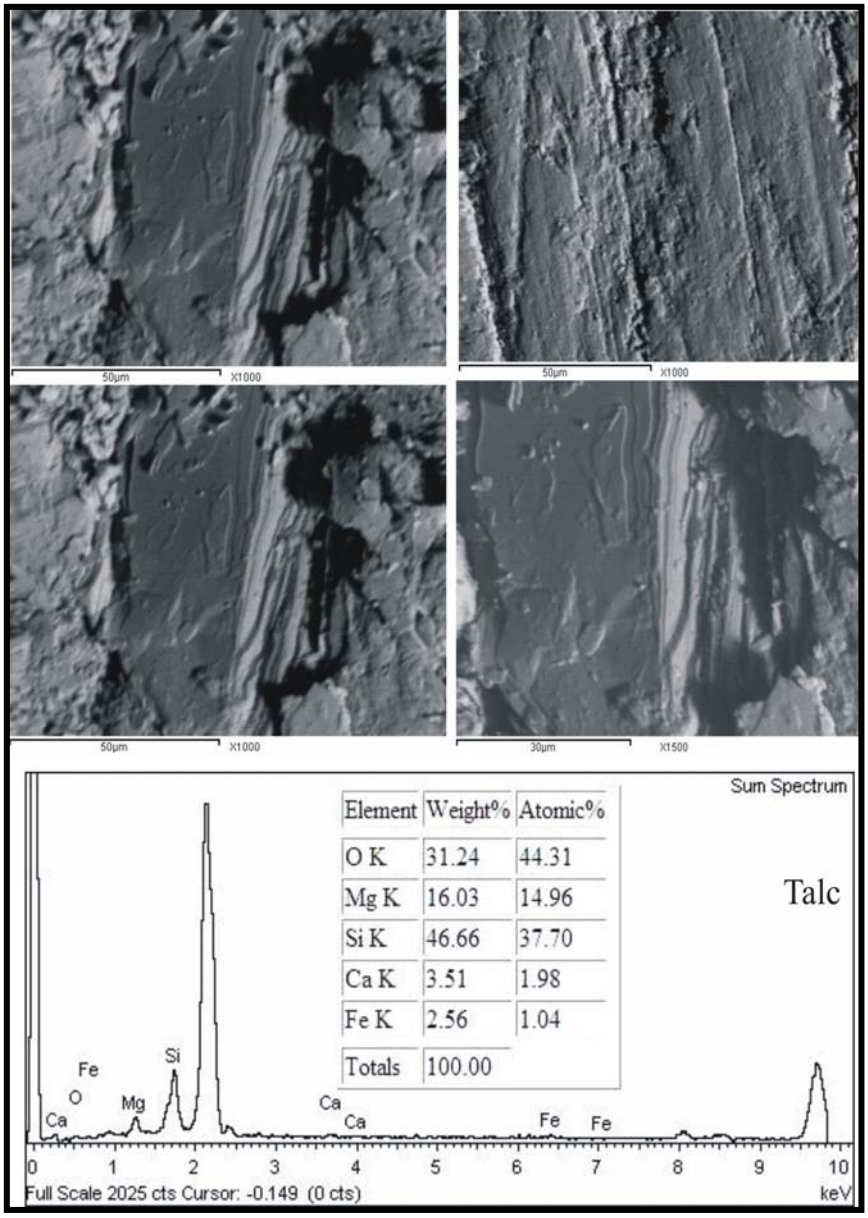

Fig.42: Close up view of SEM photomicrograph showing idiomorphic to subidiomorphic crystals of talc and its EDAX spot micro-analyses.

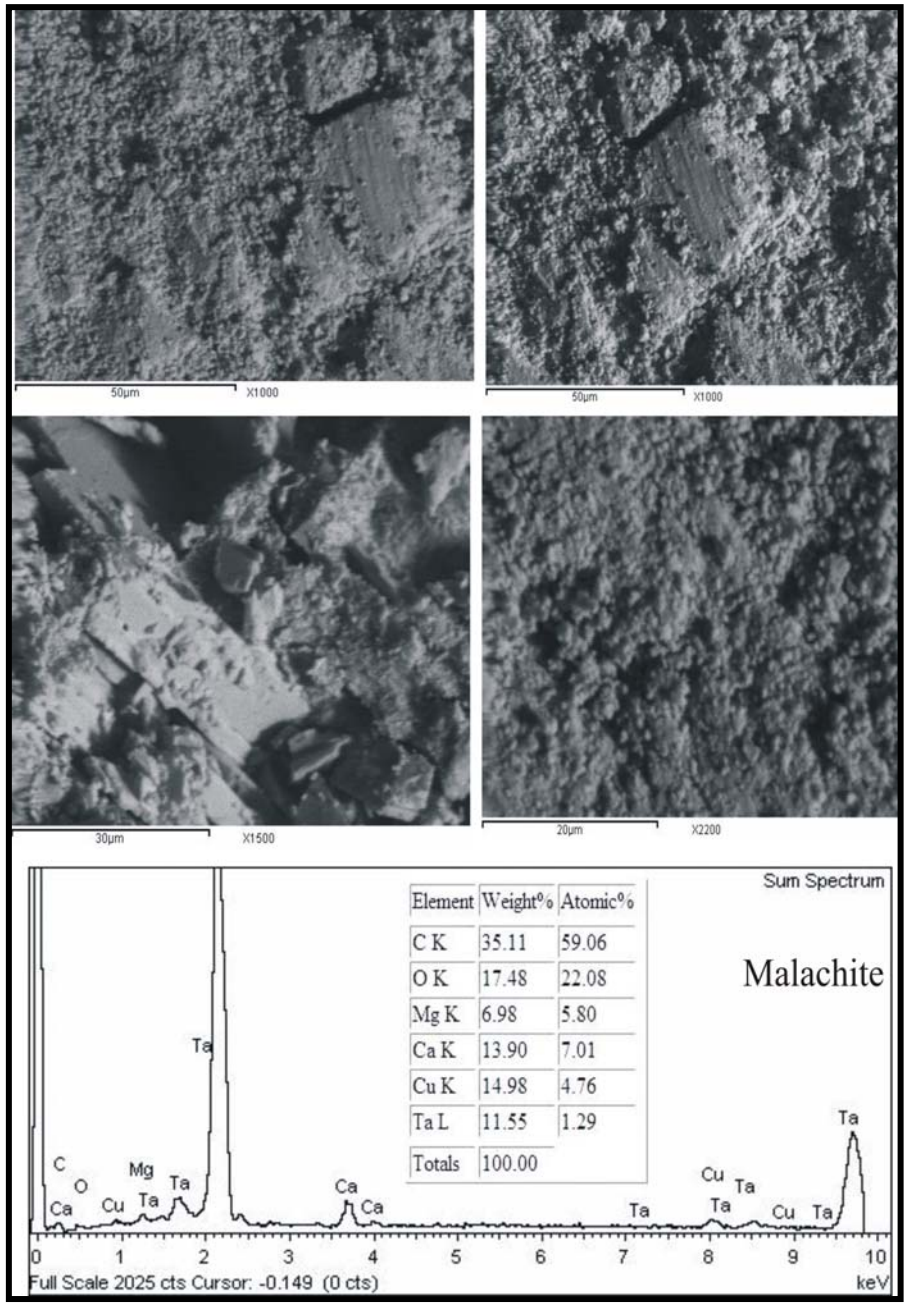

Fig.43: Close up view of SEM photomicrograph showing subidiomorphic crystals of malachite and its EDAX spot micro-analyses.

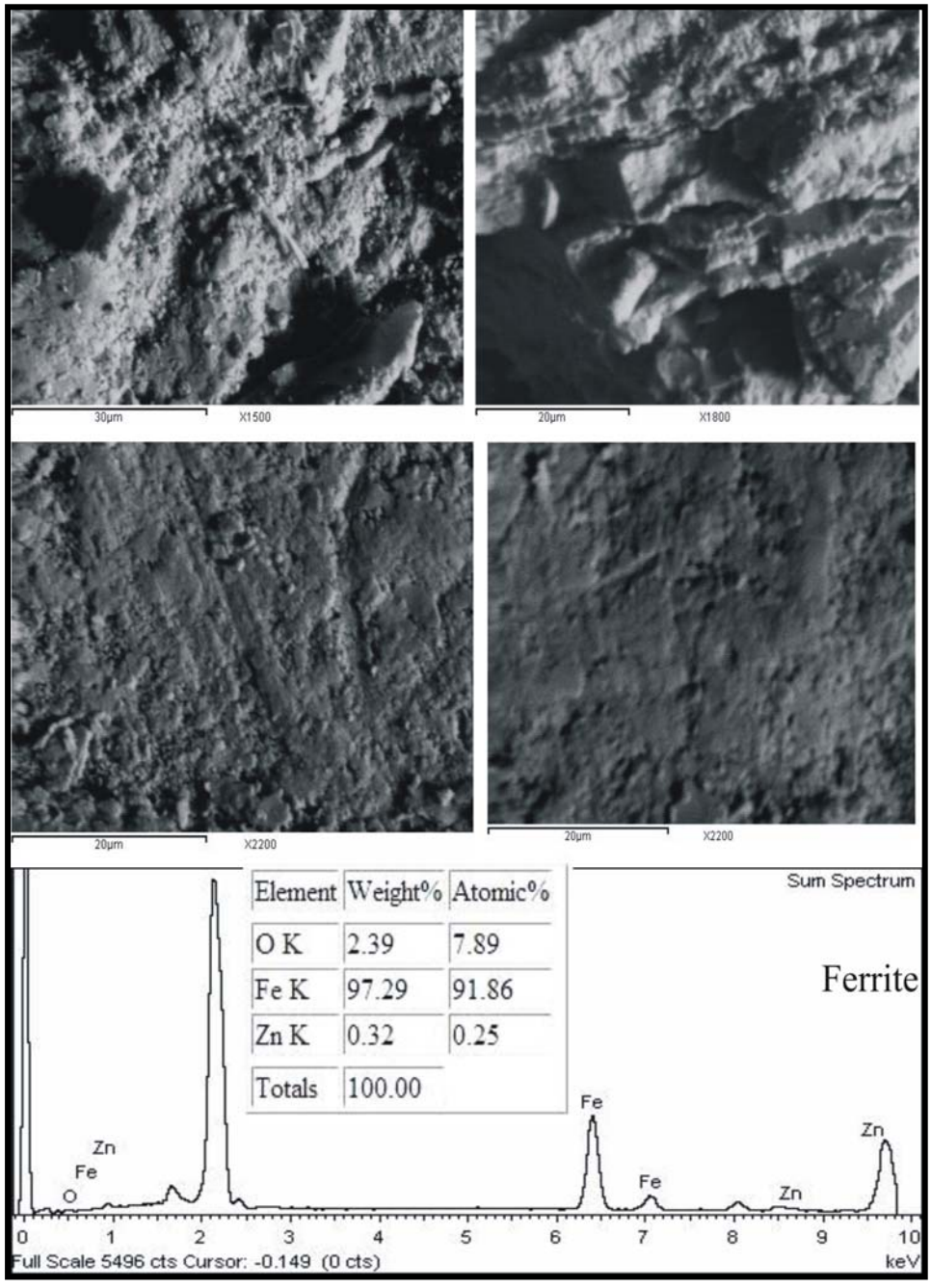

Fig.44: Close up view of SEM photomicrograph showing xenomorphic crystals of ferrite and its EDAX spot micro-analyses.

The degree of whiteness reflects to some extent the purity of the talc, as it decreases with increasing amount of impurity oxides such as Al_2O_3, CaO, FeO and Fe_2O_3.

The harmful elements (As, Zn, Zr, Co and Cu) are low except for a few samples, so that the talc should have a wide range of uses in industry without treatment. The talc products have whiteness of less than 90%, which is appropriate for use in the paint industry, but the talc would require considerable processing before being acceptable to the paper, paint and cosmetics industries.

The pure talc ore is of economic importance, while the properties and qualities of the other ore types do not meet the industrial specifications.

9. Conclusions

Talc is a soft hydrated magnesium silicate that occurs as fine platelets used in the production of ceramics and refractories. Talc carbonate occurrences were discovered in the Umm Rilan area, embedded in the Pan-African ophiolitic rocks of the Late Proterozoic.

Umm Rilan talc carbonate deposits occur along the shear zone in the ultramafic-mafic rocks which were affected by hydrothermal solutions rich in magnesium. They show preferred orientation where they fall within a plane striking 110° 130° and dipping 50° 60 NE°. Talc lenses and pockets are pure of high quality, compact, white to pale green, foliated or platy texture and occasionally stained by malachite and manganese.

Talc shows two crystal forms reflecting two modes of occurrences. The first is fine shreds which perhaps formed as a result of talcification of serpentine minerals in ultramafic rocks and amphibole minerals in mafic rocks. The second mode is coarse platy crystals. The contents of the impurity oxides in the talc deposits (FeO, Fe_2O_3, CaO, Na_2O, K_2O and Al_2O_3) are high (up to 15%). The average Fe/(Fe+Mg) ratio in the talc deposits is very low (0.11%).

Talc-carbonate rocks microscopically, consist mainly of talc, malachite, dolomite, tremolite and magnesite. X-ray diffraction analysis revealed that, these rocks are composed of talc, dolomite, magnesite, gismondite and antigorite confirming the results of the microscopic studies.

Geochemically, these rocks exhibit mafic-ultramafic cumulate ophiolite rocks, metamorphic peridotite and dunite in composition. The different variation diagrams indicate that these rocks originated from cumulative komatiite with tendency to be of tholeiitic magma and revealed that these rocks formed in low Ti-ophiolites of tholeiitic environment.

The scanning electron microscopic analysis detected presence of Ta, Zn and Fe minerals in association with Cu, Ca and Mg mineralization. The contents of Cu, Zn and Pb show that high tendency to be concentrated in the hydrothermally altered products associated with the sulfide minerals. The grade of metamorphism of these talc-carbonate rocks is the low grade of greenschist facies and was formed under low to medium pressure, low temperature of low Al_2O_3/CaO values. Umm Rilan talc-carbonates are of hydrothermal origin.

Tectonic activity plays a major role in the formation of Umm Rilan talc deposits by allowing fluids to penetrate rocks, creating a micro-permeability that facilitates reactions with the host rock. In ultramafic rocks talc as lenticular veins commonly occurs along shear zone planes.

In the studied area, at lower temperatures in the greenschist facies, both tremolite and antigorite may be converted to talc by CO_2 metasomatism, but at still lower temperatures talc is unstable in the presence CaO and CO_2, and is replaced by magnesite. Access of H_2O and CO_2 to ultramafic rocks is demonstrated by the conversion of serpentinites to rocks consisting of talc + magnesite + dolomite. Introduction of H_2O and a small amount of CO_2 has often resulted in rims of talc + magnesite enclosing serpentinites. The most important alteration of matter that can be demonstrated is an increase in the contents of H_2O and CO_2, but there is no direct relationship between their ratios. Segregation of magnesium and the origin of talc, indicates that transfer of substances also participates in serpentinization.

References

1. Abdel Kader, Z. and Shalaby, I.M., 1982. Post ore alteration at the Atshan talc mine, Hamata, Eastern Desert, Egypt. Ann. Geol. Surv. Egypt 12: 163-175.
2. Aumento, F. and Laubat, H. 1971: The Mid-Atlantic ridge near 45 N. Serpentinized ultramafic intrusions. Can. J. Earth Sci. Vol. XVI, 8, P. 531-863.
3. Barth, T.F.W. 1962. Theoretical petrology-John Wiley and Sons, New York.

4. Bowen, N.L. and Tuttle, O.F., 1949. The system SiO2-H2O-MgO. Bulletin Geological Society American. Volume 60, pp. 439.
5. Braun, P.B., 1957. Crystal structures of a new group of ferromagnetic compounds. Philips Research Reports, 12, 491-548.
6. Coleman, R.G., 1977. Ophiolites, Ancient Oceanic Lithosphere. Springer-Verlag, Berlin, Heidelberg.
7. Deer, W.A., Howie, R.A., Zussman, J., 1992. An Introduction to the Rock-forming Minerals. Longman, London, 696 p.
8. El-Kazzaz, Y.A., 1995. Tectonics and mineralization of Wadi Allaqi, South Eastern Desert, Egypt. Ph.D. thesis, University of Luton, England, UK, pp. 220.
9. Hallberg J.A., 1985. Geology and mineral deposits of the Konora-Iaverton area, northeastern Yilgam block, Western Australia, 140 p. Hesperian Press, Perth, Western Australia.
10. Hassan, K.E.K., 1969. Geology of the area around Hamata talc mine, Eastern Desert. Ph.D. Thesis, Assiut University.
11. Hussein, A.A., 1990. Mineral deposits of Egypt. In: Said, R. (Ed). The geology of Egypt. Elsevier, Amsterdam, pp 511-566.
12. Hynes, A., 1982. A comparison of amphiboles from medium and low pressure metabasites. Cont. Mineral. Pet., V. 81, p. 119-125.
13. Irvine, T.N., and Baragar, W.R.A., 1971. A guide to the chemical classification of the common volcanic rocks. Can. Jour. Earth. Sc. 8, 523-548p.
14. Le Maitre, R.W., 1989. A classification of igneous rocks and glossary of terms recommendation of the international union of geological sciences subcommision on the systematic of the igneous rocks. Blackwell Sci. Bull. Oxford, London, pp.171.
15. Mehnert, K.R., 1968. Migmatites and the origin of granitic rocks. Elsevier Publishing, Amesterdam, London, New York.
16. Mével, C., 2003. Serpentinization of abyssal peridotites at mid-ocean ridges. C.R. Geosci. Paris 335, 825–852.
17. Miyashiro, A., 1974. Volcanic rock series in island arcs and active continental margins. Am. Jour. Sci., v. 274, pp. 321-355.
18. Müller, W.F., Schmädicke, E., Okrush, M., Schüssler, U., 2003. Intergrowths between anthophyllite, gedrite, calcic amphibole, cummingtonite, talc and chlorite in a metamorphosed ultramafic rock of the KTB pilot hole, Bavaria. Eur. J. Miner. 15 (2), 295–307.

19. Nasr, B.B. and Masoud, M.S., 1999. Geology and genesis of Wadi Allaqi talc deposit, South Eastern Desert, Egypt. Annals Geol. Surv. Egypt. V. XXII, pp. 309-317.

20. Niggli, P.1954. Rocks and Mineral Deposits-Freeman, San Francisco.

21. Pearce, J.A., 1975. Basalt geochemistry used to investigate past environments on Cyprus, tectonophysics, V. 25, pp. 41-67.

22. Pfeifer, H.R., 1979. Fuid-Gestein-Interaktion in metamorphen ultramafititen der Zentral Alpen. Ph.D. Thesis, ETH-Zurich. No. 6379. Zurich, Switzerland.

23. Rashwan, A.A., Taylor, W.E.G. and Hamed El-Kazzaz, Y.A., 1995. Geological and structural evolution of Wadi Umm Rilan area Southeastern Desert, Egypt. Proc. Inter. Conf. 30 Years Cooper, P. 188, abstract.

24. Rasse, P., 1974: Al and Ti contents of hornblende, indicators of pressure and temperature of regional metamorphism. Contrib. Mineral. Petrol., V. 45, pp. 321-236.

25. Raymond, L.A., 1995. The study of igneous, sedimentary and metamorphic rocks. Wm. C. Brown Communications, Inc., USA, 498p.

26. Rock, N.M.S., 1990. The International Mineralogical Association (IMA/ CNMMN) pyroxene nomenclature scheme: Computerization and its consequences Mineralogy and Petrology, 4 3, 99- 119.

27. Said, R., 1962. The geology of Egypt. Elsevier, Amsterdam, 377 pp.

28. Salem, I.A., 1992. Talc deposits at Rod El-Tom and Umm El-Dalalil areas, Eastern Desert, Egypt. Egypt J. Geol. 36 (1-2): 175-189.

29. Salem, I.A., Aly, S.M., Scott, P. and El-Sharkawy, M.F., 1999. Genetic relationship between volcanogenic massive sulphide and talc mineralizations at Darhib area, Eastern Desert, Egypt. Egyptian Mineralogist, volume 11, pages 110-134.

30. Serri, G., 1981. The petrochemistry of ophiolite-gabbroic rocks complexes: A key for the classification of ophiolites into low-Ti and high-Ti types, Earth Planet. Soc. Lett. 52: pp. 203-212.

31. Schandl, E.S., Gorton, M.P., Sharata, N.A., 2002. The origin of major talc deposits in the Eastern Desert of Egypt: relict fragments of metamorphosed carbonate horizon? J. Afr. Earth Sci. 34, 259–273.

32. Winkler, H.G.F., 1976. Petrogenesis of metamorphic rocks. 4th, edition. Springer-Verlage. Berlin-Heidelberg-New York, 342p.

33. Zakrutkin, V. 1968: The evolution of amphibolites during metamorphism. Vsesoyuzone (USSR), Mineralogicheskoe obschestov, Zapiski (Verhandlungen), Vol. 97: p. 13-23.